Available online at www.sciencedirect.com
SCIENCE DIRECT®
Journal of Crystal Growth 263 (2004) 251–255
JOURNAL OF CRYSTAL GROWTH
www.elsevier.com/locate/jcrysgro

Growth and optical properties of $0.62Pb(Mg_{1/3}Nb_{2/3})O_3$-$0.38PbTiO_3$ single crystals by a modified Bridgman technique

Xinming Wan[a,b,*], Jie Wang[b], H.L.W. Chan[b], C.L. Choy[b], Haosu Luo[a], Zhiwen Yin[a]

[a] *The State Key Laboratory of High Performance Ceramics and Superfine Microstructure, Shanghai Institute of Ceramics, Chinese Academy of Sciences, 215 Chengbei Rd. Jiading, Shanghai 201800, China*
[b] *Department of Applied Physics, The Hong Kong Polytechnic University, Hung Hom, Hong Kong, China*

Received 29 September 2003; accepted 6 November 2003
Communicated by M. Schieber

Abstract

Large size 0.62PMN-0.38PT single crystals with high optical quality have been grown by a modified Bridgman technique. X-ray diffraction shows they have tetragonal phase and are free of pyrochlore phase. The melting point and thermal stability of the as-grown crystals were measured using simultaneous thermo-gravimetric analysis and differential thermal analysis. The optical transmission spectra from 0.3 to 11 μm of a ⟨0 0 1⟩-cut 0.62PMN-0.38PT single crystal were studied at room temperature. The extinction ratio is also measured from 20°C to 70°C. The wide transparent region (from 0.45 to 5.5 μm) and high optical transmittance (about 70%) indicate that the crystals can be used in a very wide wavelength region. The high extinction ratio, which is independent of temperature is an important property for optical device application. Some discussions about the oxygen-octahedra structure that determines the basic energy level of the crystals are also presented in this paper.

Keywords: A1. Absorption edge; A1. Extinction ratio; A1. Optical transmittance; A2. Bridgman technique; B1. 0.62PMN-0.38PT single crystals

1. Introduction

Bulk single crystals of relaxor ferroelectric $(1-x)Pb(Mg_{1/3}Nb_{2/3})O_3$–$xPbTiO_3$ (PMN-PT) have come into prominence due to their unusually large dielectric and piezoelectric properties in contrast to conventional piezoelectric ceramics [1–3]. For example, 0.67PMN-0.33PT single crystals, whose composition is near the morphotropic phase boundary (MPB), show an ultrahigh piezoelectric constant ($d_{33} \sim 2500$ pC/N), permittivity ($\varepsilon_r \sim 5000-5500$) and electromechanical coupling factor in the longitudinal bar mode ($k_{33} \sim 94\%$) [4,5]. These values are much higher than that of $d_{33} \sim 700$ pC/N and $k_{33} \sim 70-80\%$ in conventional $Pb(Zr,Ti)O_3$(PZT) ceramics [6,7], which have been widely used in ultrasonic transducers and strain actuators in the past 40 years [8].

Although most recent research on PMN-PT has focused on its unusually large piezoelectric

*Corresponding author. Tel.: +86-852-2766-4616; fax: +86-852-2333-7629.
E-mail address: xmwan@citiz.net (X. Wan).

0022-0248/$ - see front matter
doi:10.1016/j.jcrysgro.2003.11.053

response, this material has recently also been found to exhibit extremely large electro-optic coefficients, with $r_{33} = 207\,\text{pm/V}$ ($\lambda = 632.8\,\text{nm}$) for $\langle 0\,0\,1\rangle$-poled 0.67PMN-0.33PT, 107 pm/V for $\langle 1\,1\,1\rangle$-poled 0.67PMN-0.33PT, and $r_{33} = 70\,\text{pm/V}$, $r_{51} = 558\,\text{pm/V}$ for $\langle 0\,0\,1\rangle$-poled 0.62PMN-0.38PT [9]. The results show that PMN-PT single crystals are also promising candidates for optical devices. Although PMN-PT single crystals can be grown relatively easily by many groups, these crystals cannot be used as optical crystals for their poor quality. The small size and poor optical transmittance restrict its further investigation and applications. Recently, we have grown larger size 0.62PMN-0.38PT single crystals by a modified Bridgman technique, and their performance has been characterized. The results show that 0.62PMN-0.38PT single crystals have good optical properties in a wide range of wavelengths.

2. Experimental procedure

The ferroelectric 0.62PMN-0.38PT single crystals have been grown by a modified Bridgman technique [10,11]. The raw powders of PbO, MgO, Nb_2O_5 and TiO_2 with purity more than 99.99% are used as the starting materials. To prevent formation of the pyrochlore phase during crystal growth, the raw materials were precalcined by the B-site precursor synthesis method [12]. Then the powders were put into a platinum crucible, which was sealed to prevent the evaporation of lead. The 0.67PMN-0.33PT single crystals were used as seed crystals. The crystal seeds had a key effect on restraining spontaneous nucleation and parasitic growth.

During the crystal growth, the highest solution temperature is usually more than 100°C above its melting point and the temperature gradient is about 30–50°C/cm at the solid–liquid interface. The temperature in the Bridgman furnace was regulated by a proportional integral differential (PID) controller. The precision of the furnace temperature was controlled within ± 0.5°C. The growth temperature profile used was rapid heating to 1350°C, after soaking for about 10 h, the crucible was pulled down at a rate of 0.1–1.0 mm/h. Finally, the furnace temperature was decreased at a rate of 25°C/h to room temperature and the crucibles were weighed to evaluate the weight loss of contents during the crystal growth. Usually 0.62PMN-0.38PT single crystals with a size of about $\varnothing\ 48 \times 80\,\text{mm}$ could be obtained.

The melting point and thermal stability of the resulting crystals were measured using simultaneous thermo-gravimetric analysis (TG) and differential thermal analysis (DTA). In order to confirm the phase, single crystals were ground into fine powder for X-ray diffraction (XRD) analysis.

In this work, all the samples were oriented and cut along the $\langle 0\,0\,1\rangle$ direction as confirmed by XRD. Silver paste was painted on the sample surfaces and sintered at 580°C for 30 min. Then, the samples were poled along the $\langle 0\,0\,1\rangle$ direction under an electric field of 10 kV/cm for 15 min near their T_m in silicone oil and then slowly cooled to room temperature while maintaining the half of the applied electric field.

For optical characterization, the surfaces for light transmitting were polished using alumina and diamond polishing compounds (with decreasing average grit size down to 0.05 μm) to achieve highly polished quality. The samples were finally polished into a thickness of 0.7 mm. For transmission measurement, the incident light was perpendicular to the $\langle 0\,0\,1\rangle$ surface, i.e. propagation along the $\langle 0\,0\,1\rangle$ direction. Transmission spectra were measured at room temperature as a function of wavelength. A Shimadzu UV-2501PC Spectrophotometer with the wavelength range from 200 to 800 nm and a ThermoNicolet Nexus 870 Fourier-transform-infrared (FT-IR) spectrophotometer with the wavelength range from 2.5 to 25 μm were used.

3. Results and discussions

3.1. Crystal structure and thermal stability

Fig. 1 shows the 0.62PMN-0.38PT single crystals obtained by a modified Bridgman technique using seed crystals. The crystal boules are 48 mm in diameter and about 70 mm in length.

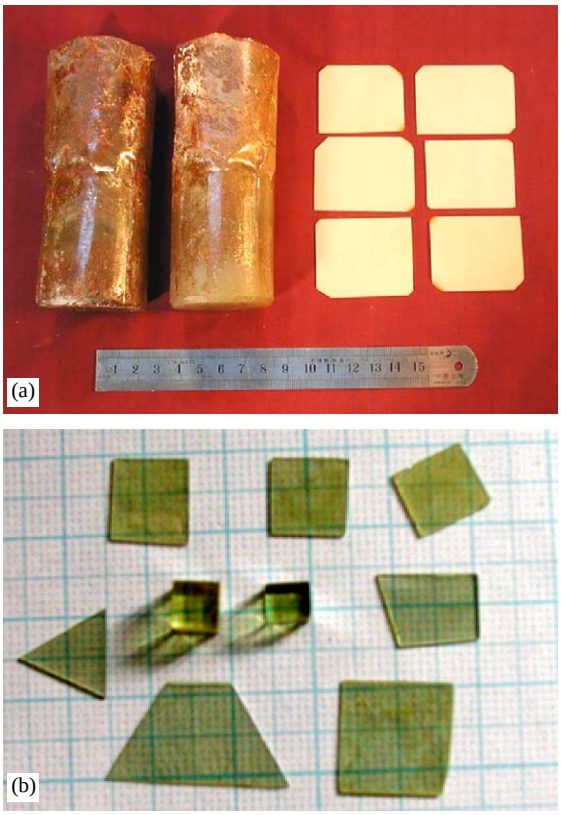

Fig. 1. The 0.62PMN-0.38PT crystals obtained by a modified Bridgman technique. (a) As-grown crystal boules (b) After being poled and polished.

They are light yellow in color and more transparent than 0.67PMN-0.33PT or 0.70PMN-0.30PT single crystals, which have been investigated widely. There are still some cracks in the crystals presumably caused by stress brought about by the lattice deformation during phase transition and by the thermal gradient during crystal growth. But the size and quality of the crystals are good enough for various applications, even for optical devices. The samples including some crystal ingots and some sectional crystal slices are shown in Fig. 1(b). The thickness of these crystal slices varies from 0.6 to 1.2 mm and they are transparent.

The 0.62PMN-0.38PT single crystals are expected to have a tetragonal phase at room temperature [13] and the spontaneous polarization is along the $\langle 0\,0\,1 \rangle$ direction (c-axis). X-ray powder diffraction analysis was used to determine the phases existed in the as-grown crystals. The sample was ground into a fine powder. The results in Fig. 2 show that the 0.62PMN-0.38PT single crystals are tetragonal and free of pyrochlore phase.

Fig. 3 shows the thermal properties of 0.62PMN-0.38PT single crystals investigated by TG and DTA. On heating, a sharp endothermic DTA peak appears at 1308°C, which corresponds to the melting of the 0.62PMN-0.38PT crystals. The TG curve indicates the high thermal stability of the crystals without significant weight loss up to 1250°C, which indicates that 0.62PMN-0.38PT single crystals can be grown directly from the melt by a Bridgman technique.

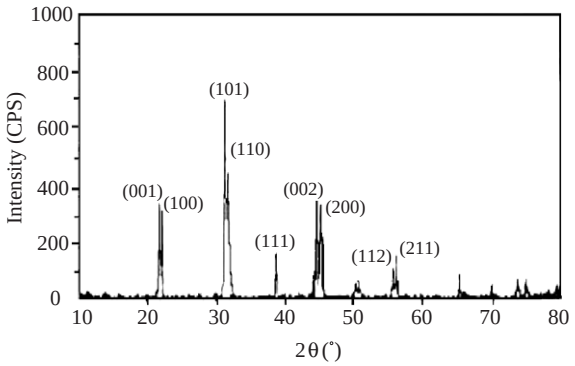

Fig. 2. XRD patterns for 0.62PMN-0.38PT single crystals.

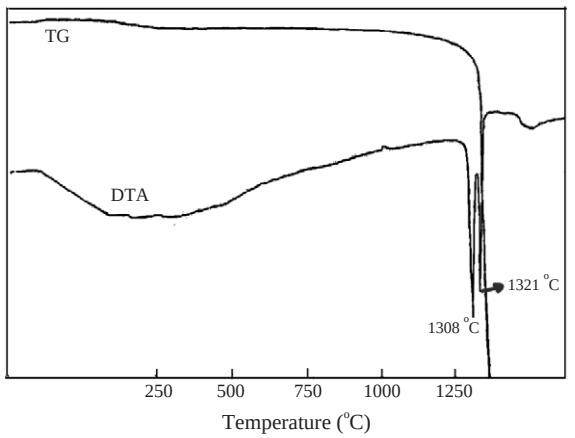

Fig. 3. A simultaneous TG and DTA curves for 0.62PMN-0.38PT single crystals.

3.2. Optical properties

Fig. 4 shows the transmission spectra of 0.62PMN-0.38PT single crystals with the wavelength varies from 0.3 to 11 μm. Under a poled condition, the crystal is transparent between 0.45 and 5.5 μm and the transmission rolls off near 450 nm. The sample becomes completely absorbing around 400 nm in the near UV region and at 10 μm in the infrared region. But the wavelength cutoff in the near UV is much sharper than the long wavelength cutoff [14]. This is similar to most oxygen-octahedral perovskites. As compared with unpoled condition, we can conclude that the sample does not go through a phase transition during the poling process because it has the same optical absorption edge before and after poling. But the transmission has increased dramatically after poling. On the surface and the domain walls of the crystal, the refractive index has a discontinuity, which will reduce the transmission. The unpoled sample obviously has many domain walls and nanoregions with different orientations with respect to the optic axis. When the incident light passes through the crystal, those domain boundaries cause multiple scattering and generate larger scattering losses. For tetragonal 0.62PMN-0.38PT single crystal, the spontaneous polarization is along the ⟨0 0 1⟩ direction. After poling the sample along ⟨0 0 1⟩ direction, the single domain area enlarges and the losses due to the domain walls reduce substantially.

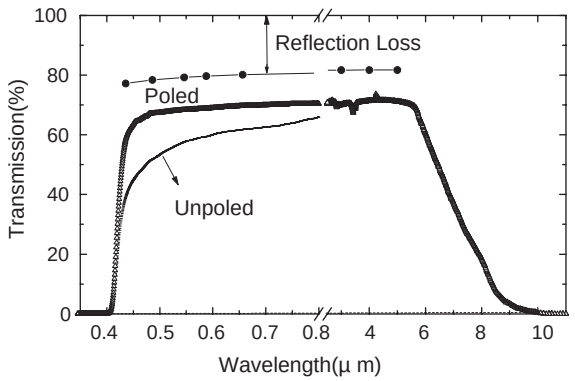

Fig. 4. The transmission characteristics of ⟨0 0 1⟩-oriented 0.62PMN-0.38PT (the wavelength region is 0.3–11 μm for poled condition and 0.3–0.8 μm for unpoled condition) (see Ref. [14]).

From the transmission characteristics, we can see that the optical absorption is very small in the 0.45–5.5 μm wavelength range for the poled condition. In general, the optical transmission relates to reflection and scattering losses. With the modified Sellmeier's equation of 0.62PMN-0.38PT single crystal reported by us in another article [15]:

$$n^2(\lambda) = 6.2144 + \frac{0.2151}{\lambda^2 - 0.0686} - 0.0004 \times \lambda^2. \quad (1)$$

The refractive index between 0.45 and 5.5 μm can be calculated. Using the Fresnel expression

$$R = \frac{(n-1)^2}{(n+1)^2}. \quad (2)$$

The reflection losses of the light at two surfaces were calculated and are also shown in Fig. 4. After considering the reflection losses at both surfaces, the transmission from 0.45 to 5.5 μm wavelength region is quite high and the crystals can be used as optical crystals in a very wide wavelength region.

We also measured the extinction ratio of a ⟨0 0 1⟩-cut 0.62PMN-0.38PT single crystal with a 4 mm long cube. The extinction ratio is about 28 dB at room temperature. Fig. 5 presents the temperature dependence of the extinction ratio of the sample. We can see that the extinction ratio of the crystal changes only slightly from 20°C to 70°C. The high extinction ratio is independent of

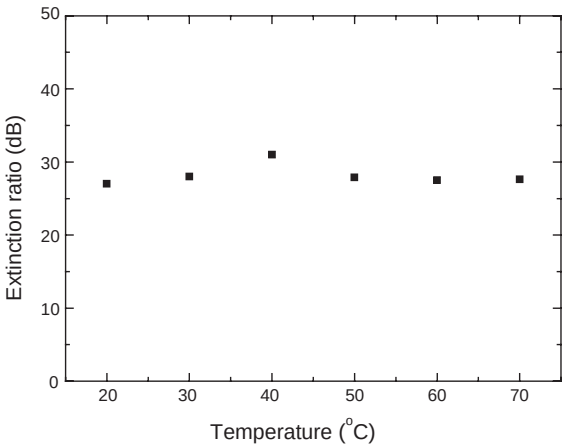

Fig. 5. Temperature dependence of extinction ratio for 0.62PMN-0.38PT single crystals.

temperature, which is an important property for use in optical devices.

0.62PMN-0.38PT single crystal, like other ABO_3-type perovskite compounds, such as PMN, PMNT, PZNT family, has a common oxygen-octahedra structure that determines the basic energy levels in the crystal [16–18]. In $Pb(B_1B_2)O_3$ ferroelectric relaxors, the nanoregions, domain structure and B-site cation structure have influences on the transmittance as well as on the dielectric and piezoelectric behavior of the crystal. For 0.62PMN-0.38PT, the Mg^{2+}, Nb^{5+} and Ti^{4+} ions occupy the same crystallographic site in the structure and the crystal has a complex energy distribution. The distortion of lattice, ion vibration and interaction of the ions with different poling directions give rise to complex mechanisms which influence the optical properties of the crystal.

4. Conclusions

Large size and high optical quality crystals of 0.62PMN-0.38PT single crystals have been grown by a modified Bridgman technique using a seed crystal. X-ray diffraction shows that the as-grown 0.62PMN-0.38PT single crystals are tetragonal and free of pyrochlore phase. The melting point and thermal stability of the crystals were measured using simultaneous thermo-gravimetric analysis (TG) and differential thermal analysis (DTA).

The optical transmission spectra from 0.3 to 11 μm of a $\langle 0\,0\,1\rangle$-cut 0.62PMN-0.38PT single crystals were studied at room temperature. The crystal is transparent between 0.45 and 5.5 μm and the optical transmittance in this region is about 70%. They become completely absorbing around 0.4 μm in the near UV region and at 10 μm in the infrared region. But the wavelength cutoff at 0.4 μm is much sharper than the long wavelength cutoff. The wide transparent region and high optical transmittance indicate that the crystals can be used in a very wide wavelength region. The extinction ratio of the 0.62PMN-0.38PT single crystal with a 4 mm long cube is also measured. It is about 28 dB at room temperature and changes only slightly from 20°C to 70°C. The temperature-independent high extinction ratio is an important property when the crystals are used for optical devices.

Acknowledgements

This work is supported by the National Natural Science Foundation of China (Grant No. 50272075), the High Technology and Development Project of the People's Republic of China (Grant No. 2002AA325130) and Hong Kong Research Grants Council (PolyU 5193/00P), the Centre for Smart Materials of the Hong Kong Polytechnic University. The authors are thankful to Dr. Hu Cao of Montana State University in USA.

References

[1] F. Robert, Service Sci. 275 (1997) 1878.
[2] Z.W. Yin, H.S. Luo, P.C. Wang, G.S. Xu, Ferroelectrics 229 (1999) 207.
[3] S.-E. Park, T.R. Shrout, J. Appl. Phys. 82 (1997) 1804.
[4] S.-E. Park, T.R. Shrout, IEEE Trans. Ultrason. Ferroelectr. Freq. Con. 44 (1997) 1140.
[5] G. Xu, H. Luo, P. Wang, H. Xu, Z. Yin, Chin. Sci. Bull. 45 (2000) 491.
[6] K. Harada, S. Shimanuki, T. Kobayashi, S. Saitoh, Y. Yamsshita, J. Am. Ceram. Soc. 81 (1998) 2785.
[7] K. Harada, S. Shimanuki, T. Kobayashi, S. Saitoh, Y. Yamsshita, Key Eng. Mater. 157 (1999) 95.
[8] J. Yin, W. Cao, J. Appl. Phys. 87 (2000) 7438.
[9] D.-y. Jeong, Y. Lu, V. Sharma, Q. Zhang, H.-s. Luo, Jpn. J. Appl. Phys. 42 (2003) 4387.
[10] H.S. Luo, G.S. Xu, P.C. Wang, Z.W. Yin, Ferroelectrics 231 (1999) 97.
[11] H.S. Luo, G.S. Xu, P.C. Wang, H.Q. Xu, Z.W. Yin, Jpn. J. Appl. Phys. 39 (2000) 5581.
[12] M. Orita, H. Satoh, K. Aizawa, Jpn. J. Appl. Phys. 31 (1992) 3261.
[13] T.R. Shrout, Z.P. Chang, N. Kim, S. Markgraf, Ferroelectr. Lett. 12 (1990) 63.
[14] X. Wan, H. Luo, J. Wang, H.L.W. Chan, C.L. Choy, Solid State Commun. 129 (2004) 401.
[15] X. Wan, H. Xu, T. He, D. Lin, H. Luo, J. Appl. Phys. 93 (2003) 4766.
[16] M. DiDomenico Jr., S.H. Wemple, J. Appl. Phys. 40 (1969) 720.
[17] Y.H. Bing, R. Guo, A.S. Bhalla, Ferroelectrics 242 (2000) 1.
[18] S. Nomura, H. Arima, F. Kojima, Jpn. J. Appl. Phys. 12 (1973) 531.